Comparative Experimental Study of the Annular Ellipsoidal and Rectangular Layouts MOSFETs in X-ray Ionizing Radiation Environments

William S. Cruz
Departamento de Engenharia Elétrica
Centro Universitário da FEI
Brazil
williamcruz@fei.edu.br

Salvador P. Gimenez
Departamento de Engenharia Elétrica
Centro Universitário da FEI
Brazil
sgimenez@fei.edu.br

ABSTRACT

This paper presents a comparative study of the Total Ionizing Dose (TID) effects between the different layouts styles for Metal-Oxide-Semiconductor Field Effect Transistors (MOSFETs), the Annular Ellipsoidal Gate MOSFET (AEGM) and the Rectangular MOSFET (RM), regarding the same gate area and bias conditions. The devices were manufactured by using 180 nm Bulk process of Taiwan Semiconductor (TSMC). The results show that the AEGM is capable of supporting a TID of up to 6 Mrad without variations that compromise its electrical operation, while for the same TID, its rectangular counterpart has completely stopped working properly for these devices.

KEYWORDS

Annular Ellipsoidal Gate MOSFET, TID, layouts styles for MOSFET

1 INTRODUCTION

With the constant evolution of electronics and following Moore's Law, several efforts have been made in search of new manufacturing methods, new structures or materials that suit the MOSFETs devices to the increasingly smaller dimensions and still, maintain their analog and digital electrical characteristics [1]. Within that context, a new very innovative and unexplored technique is the use of different gate geometries for the MOSFETs devices [2]. With the change of conventional geometry, new effects are found that contribute to the improvement of important parameters of the study device, such as Longitudinal Corner Effect (LCE), Parallel Connection of Different MOSFETs with Different channel Lengths Effect (PAMDLE) or Deactivation of Parasitic MOSFETs in the Bird's Beak Regions Effect (DEPAMBBRE) [3-7]. This differentiated strategy also does not add any cost to the current and established manufacturing processes of Complementary Metal-Oxide-Semiconductor (CMOS) integrated circuits (ICs). Examples of this type of approach are the MOSFETs hexagonal (Diamond), octagonal (Octo), ellipsoidal, wave and fish [3-7].

Some recent studies of these technologies present how much each of them can be better compared to those conventionally used, such as the increasing drain current (I_{DS}) for the same gate area, demonstrating their potential for several applications [8-12]. Among these studies, one very important, is the robustness of these devices when subjected to ionizing radiation [9-12]. This study is of great importance for aerospace and medical areas applications, demonstrating how the effects present in some of these structures can mitigate the effects of radiation on the device, making even after a long exposure, the MOSFET continues to work with little variation in its electrical characteristics.

Following the idea of unconventional geometries and their application mainly in medical and aerospace areas, the Annular Ellipsoidal MOSFET was investigate experimentally, and thus was determined comparatively to its conventional equivalent, its tolerance to X-ray ionizing radiation.

2 LITERATURE REVIEW

2.1 The Diamond-type MOSFET

The first device to use this innovative approach was the Diamond-type MOSFET of Brazilian patent [3,9]. The main idea for the creation of this device was to use the corner effect in the longitudinal direction of the MOSFET channel, which resulted in LCE, which boosted the resulting electric field along the channel and, consequently, its electrical parameters. Another effect of this geometry is the PAMDLE, this effect has the capacity to potentiate the I_{DS}, causing the current tends to flow more by the margins of the devices, where the channel length is smaller. The DEPAMBBRE is a third effect that emerged with the application of this layout technique, this effect can electrically deactivate the parasitic MOSFETs of the bird's beak regions, through longitudinal curved electric field lines that are generated in these regions. These parasitic transistors are a huge problem when the device is subjected to ionizing radiation, because these radiations can reduce the Threshold Voltages (V_{TH}) of these parasitic MOSFETs, and with that they conduct even when the main MOSFET does not conduct.

2.2 The Octo-type MOSFET

The Octo MOSFET is an evolution of the Diamond-type and was specially developed to improve the rupture voltage and potentiate its robustness in the electrostatic discharge effect. While the Diamond MOSFET has two components of longitudinal electric field, the Octo introduces three [4,10].

Results by three-dimensional numerical simulation and experimental data prove that the Diamond and Octo layouts for MOSFETs significantly increase the performance of field effect transistors (LCE and PAMDLE) and tolerance to ionizing radiation (DEPAMBBRE) in relation to those observed when they implemented with the rectangular layout style, considering the same gate area and bias conditions [10].

2.3 Annular Ellipsoidal layout for MOSFETs

A layout not yet explored by the literature and companies of semiconductor CMOS ICs devices, is the annular ellipsoidal. This layout was based on the ellipsoidal [5,8] (which is an evolution of the Octo-type MOSFET) and Annular Circular [11] layouts. Simultaneously to other unconventional layouts, this layout can be a very interesting alternative to potentiate the electric performance of MOSFETs and its tolerance to ionizing radiation.

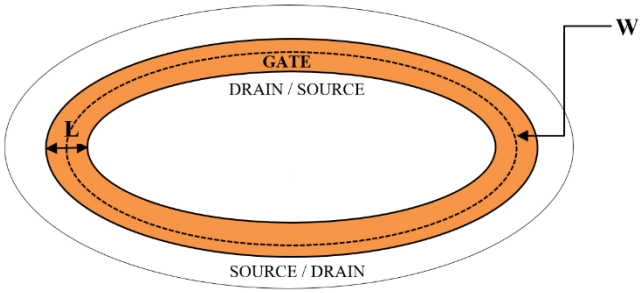

Figure 1: Example of an Annular Ellipsoidal MOSFET and the representation of its channel dimensions.

The Annular Ellipsoidal MOSFET presents a layout like that of the Ellipsoidal, but with the Source or Drain inside the ellipse.

Fig. 1 shows how the dimensions of this device are measured, being L, the channel length, what is measure of the distance between the inner and outer ellipse of the gate, and W, its width, what is the measure of the perimeter of the middle ellipse between the inner and outer ellipse of the gate. As in the Diamond, Octo and Ellipsoidal layouts, this layout has the idea of using the corner effect, enhancing the resulting electric field along the channel and, consequently, the average velocity of the mobile carriers of the channel, which leads to a better drain current (I_{DS}), transconductance (g_m), on-state resistance (R_{ON}), etc.

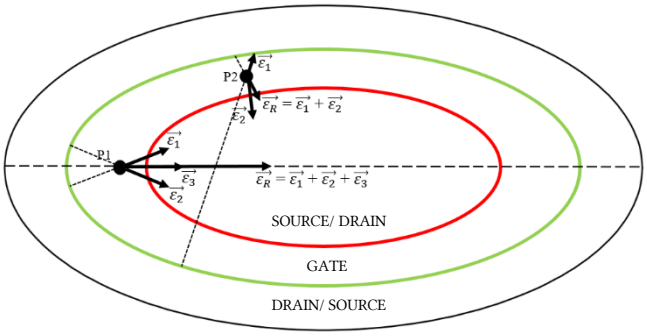

Figure 2: Simplified top view of the Annular Ellipsoidal type MOSFET, indicating the LCE and the different vector components of the longitudinal electric field ($\vec{\varepsilon_1}$, $\vec{\varepsilon_2}$ and $\vec{\varepsilon_3}$) and the resulting electric field ($\vec{\varepsilon_R}$).

In Fig. 2, analogous to what occurs in the Ellipsoidal-type MOSFET, $\vec{\varepsilon_1}$, $\vec{\varepsilon_2}$ and $\vec{\varepsilon_3}$ are the components of the longitudinal electric field at point P_1, which occur in the line defined by the focal points of the ellipsoidal geometry. Outside that line, for example in point P_2, there are only two components ($\vec{\varepsilon_1}$ and $\vec{\varepsilon_2}$), resulting from the polarization between drain and source (V_{DS}) and $\vec{\varepsilon_R}$ is the resulting vector of the longitudinal electric field.

Although this gate geometry for MOSFET does not present the DEPAMBBRE effect, it does not mean that it less robust to ionizing radiation, because the annular geometry causes these MOSFETs not to present the bird's beak regions incorporated into their structures.

3 METHODOLOGY

For the research, the devices were manufactured with the 180 nm Bulk CMOS manufacturing process of the TSMC. This circuit was fabricated via MOSIS, through the MEP program. Table 1 shows the dimensions of the MOSFETs used in this work.

Table 1: nMOSFETs Dimensions that were used to this study

Parameter	RM	AEGM
W [nm]	420	3860
L [nm]	180	260
W/L	2.3	14.8

The devices were exposed to an X-rays energy of 10 KeV by using the Shimadzu XRD-7000 diffractometer, which can generate secondary electrons with a medium range of 500 nm. Before being irradiated the MOSFETs, they were characterized by using the Keithley 4200-SCS system, through obtaining their curves I_{DS} x V_{DS} and I_{DS} x V_{GS}. With these curves and using known methods, the main figures of merits were obtained, for example, the method of the second-derived curve of the I_{DS} as a function of the gate voltage (V_{GS}) to obtain V_{TH}. The parameters obtained were: threshold voltage (V_{TH}), subthreshold slope (S), on-state drain current (I_{ON}), off-state drain current (I_{OFF}), and the ratio between these currents (I_{ON}/I_{OFF}).

During the process of X-rays ionizing radiation procedure, the MOSFETs were not biased. The chip was exposed to two doses of radiation of 3 Mrad each, with a TID of 6 Mrad with a dose rate of 23.5 krad/min or 392 rad/s. Two hours after irradiation, the MOSFETs were again electrically characterized. All electrical characterizations were carried out at room temperature.

To remove the effects of the MOSFET dimensions, the comparisons are done normalizing the electrical parameters in relation to their aspect ratios (AR).

$$AR = {}^{W}/_{L} \quad (1)$$

4 RESULTS AND DISCUSSION

Figs. 3 and 4 illustrate respectively the $I_{DS}/(W/L)$ and $I_{DS}/(W/L)$ in logarithm curves as a function of gate bias (V_{GS}) for V_{DS} equal to 100 mV, measured before and after each X-rays irradiation procedures.

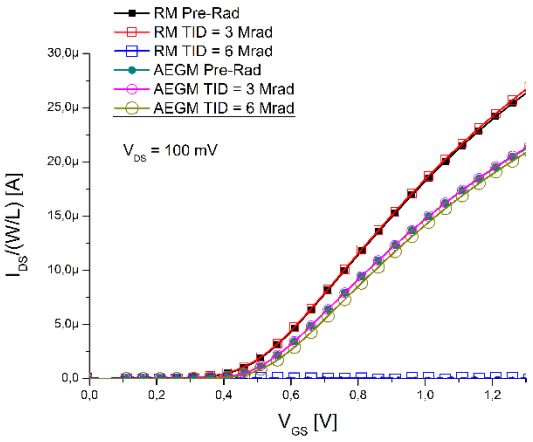

Figure 3: $I_{DS}/(W/L)$ versus V_{GS}, for V_{DS} = 100 mV, of the AEGM and RM, regarding the pre-radiation and the X-rays post-radiations.

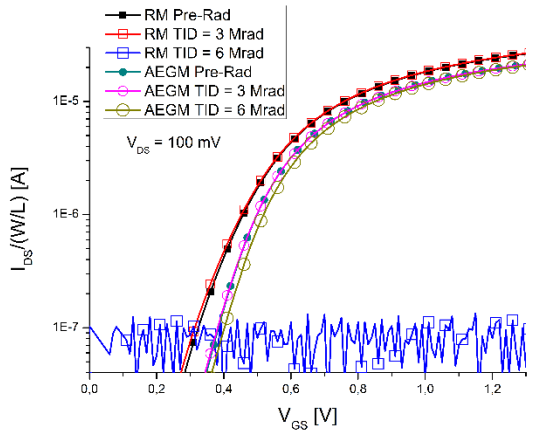

Figure 4: $I_{DS}/(W/L)$ in logarithm versus V_{GS}, for V_{DS} = 100 mV, of the AEGM and RM, regarding the pre-radiation and the X-rays post-radiations.

Based on Figs. 3 and 4, both I_{DS} of nMOSFETs practically were not affected by the TID of 3 Mrad (X-rays). However, it is observed that the RM practically crashed by a TID of 6 Mrad, while the AEGM practically does not varied due to the absence of the bird's beak regions. From Fig. 4 it also possible to note that the subthreshold slope did little to vary with a TID of 3 Mrad for both layouts.

Through Fig. 3 and using the second-derived method, V_{TH} values were found for both layouts and in each situation, these values did not have significant changes, except in the case of RM exposed to a TID of 6 Mrad, where no it was possible to extract this value, since it did not work as expected.

Figs. 5 and 6 presents respectively the RM and AEGM $I_{DS}/(W/L)$ in logarithm curves as a function of V_{GS} for V_{DS} equal to 100 mV, measured before and after each X-rays irradiation procedures. Through them the I_{ON} and I_{OFF} values were obtained for all cases.

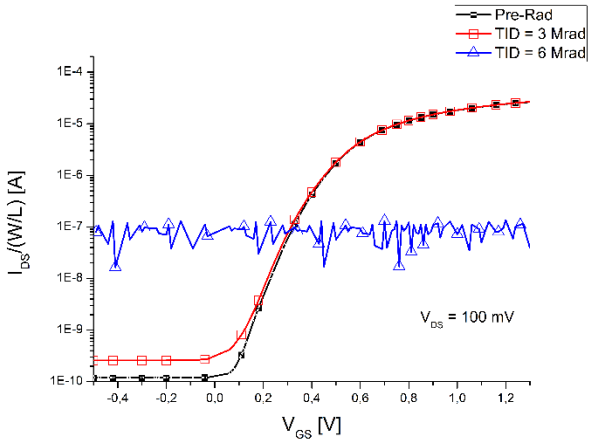

Figure 5: $I_{DS}/(W/L)$ in logarithm versus V_{GS}, for V_{DS} = 100 mV of the RM, regarding the pre-radiation and the X-rays post-radiations.

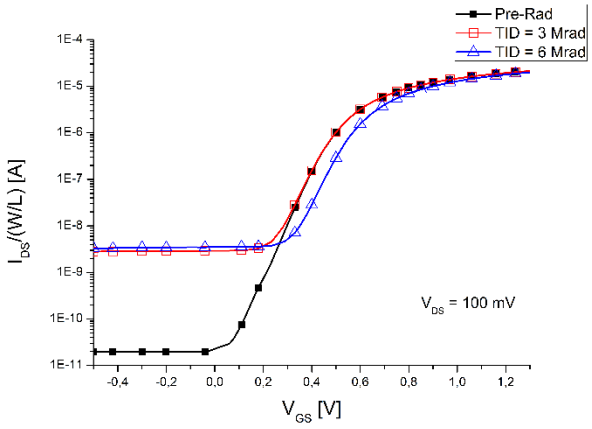

Figure 6: $I_{DS}/(W/L)$ in logarithm versus V_{GS}, for V_{DS} = 100 mV of the AEGM, regarding the pre-radiation and the X-rays post-radiations.

Analyzing Figs. 5 and 6, it is noted that although AEGM initially had a minor I_{OFF} (I_{DS} for V_{GS} = 0 V), after the first dose of ionizing radiation, this value exceeded that of the

conventional layout. That is because there was a considerable increase when taken into consideration to the increase of the RM I_{OFF} for the same dose. However, it is worth noting that after the second dose, there was a minimal variation for I_{OFF} of the AEGM, while for the RM, this current rose again, exceeding the value of the annular ellipsoidal geometry (and as mentioned affecting the functioning of the device).

In relation to the I_{ON}, both figures show little variation for a TID of 3 Mrad in both technologies, and some variation for 6 Mrad in the AEGM, considering that for the RM the value cannot be calculated, since the device left to function with such a dose.

Table 2 shows the parameters obtained through the characterization of these devices before and after each exposure to X-ray ionizing radiation, as well as their variations in relation to the value before radiation.

Table 2: Normalized parameter values analyzed as a function of the radiation doses and their variations in relation to the pre-radiation state of the conventional (RM) and Annular Ellipsoidal (AEGM) transistors

Parameter	RM			AEGM		
	Pre-Rad	3 Mrad	6 Mrad	Pre-Rad	3 Mrad	6 Mrad
V_{TH} [V]	0.48	0.48 (0%)	-	0.46	0.46 (0%)	0.47 (2%)
S [mV/déc]	88.48	90.51 (2%)	-	82.64	96.63 (17%)	98.40 (19%)
I_{ON} [μA]	16.5	17.6 (7%)	-	9.8	11.6 (18%)	11.2 (14%)
I_{OFF} [pA]	129	320 (148%)	75691 (10^5%)	22.4	2866 (10^4%)	3512 (10^4%)
I_{ON}/I_{OFF} [E+5]	1.3	0.55 (-58%)	-	4.38	0.04 (-99%)	0.03 (-99%)

Table 2 shows that AEGM presented better S and I_{ON}/I_{OFF} values initially. It is also noted that despite a greater variation of the parameters for a TID of 3 Mrad, the AEGM proved to be more robust for a TID of 6 Mrad, maintaining its operation (even more if compared only to the values after TID of 3 Mrad) while that the RM simply stopped working as a MOSFET device.

5 CONCLUSION

A comparative experimental study of the ionizing radiation effects (TID) between the AEGM and RM was performed, regarding the same bias conditions. Both devices can be considered tolerant for a TID of 3 Mrad, with the caveat that there is a considerable increase in the I_{OFF} for the AEGM. However, the AEGM practically is not affected by the X-rays ionizing radiation of 6 Mrad due to absence of the bird's beak regions, in contrast of the RM, that stopped working, regarding the same bias conditions.

ACKNOWLEDGMENTS

The authors thanks CNPq, CAPES and FAPESP for the financial support.

REFERENCES

[1] J. P. Colinge and C. A. Colinge, *"Physics of Semiconductor Devices,"* Kluwer Academic Publishers, 2002.

[2] S. P. Gimenez, *"Layout Techniques for MOSFETs,"* 1. Ed., Morgan & Claypool Publishers, 2016.

[3] Gimenez, S. P., *"Diamond MOSFET: An Innovative Layout to Improve Performances of ICs"*, Solid-State Electronics, v. 54, p. 87-88, 2009.

[4] Gimenez, S. P.; Alati, D. M., *"OCTO SOI MOSFET: An Evolution of the Diamond to Be Used In the Analog Integrated Circuits"*. In: EUROSOI 2011, VII Workshop of the Thematic Network on Silicon on Insulator Technology, Devices and Circuits. Granada: Universidade de Granada, v. 1. p. 91-92, 2011.

[5] Gimenez, S. P.; Correia, M. M.; Neto, E. D.; Silva, C. R., *"An Innovative Ellipsoidal Layout Style to Further Boost the Electrical Performance of MOSFETs,"* IEEE Electron Device Letters, v. 36, p. 705-707, 2015.

[6] Gimenez, Salvador P., *"The Wave SOI MOSFET: A New Accuracy Transistor Layout to Improve Drain Current and Reduce Die Area for Current Drivers Applications,"* Device Physics and Modeling II, ECS Transactions, 19(4): 153-158, 2009.

[7] Gimenez, S. P.; Alati, D. M.; Simoen, E.; Claeys, C., *"Fish SOI MOSFET: An Evolution of the Diamond SOI Transistor for Digital ICs Applications,"* Electron Device Physics-2, ECS Transactions, 35(5): 163-168, 2011.

[8] Silva, C. R.; Gimenez, S. P., *"Experimental Comparative Study between the Ellipsoidal and Conventional MOSFET, "* In: Seminatec, São Bernardo do Campo, São Paulo, Brasil, 2012.

[9] Seixas, L. E.; Finco, S.; Silveira, M. A. G.; Medina, N.; Gimenez, S. P., *"Study of proton radiation effects among diamond and rectangular gate MOSFET layouts,"* Materials Research Express, vol. 4, p. 015901, 2017.

[10] Fino, L. N. S.; Neto, E. D.; Silveira, M. A. G.; Renaux, C.; Flandre, D.; Gimenez, S. P., *"Boosting the total ionizing dose tolerance of digital switches by using OCTO SOI MOSFET,"* Semiconductor Science and Technology, v. 30, p. 105024-12p, 2015.

[11] Cirne, K. H.; Lima, J. L.; Seixas, L. E.; Silveira, M. A. G.; Barbosa M.; Tabacnicks, M.; Added, N.; Gimenez, S. P.; Medina, N.; Melo, W., *"Comparative Study of the Proton Beam Effects between the Conventional and Circular Gate MOSFETs,"* Nuclear Instruments & Methods in Physics Research. Section B, Beam Interactions with Materials and Atoms (Print), v. 11, p. 688-691, 2011.

[12] Souza, R. N.; Silveira, M. A. G.; Gimenez, S. P., *"Mitigating MOSFET Radiation Effects by Using the Wave Layout in Analog ICs Applications,"* Journal of Integrated Circuits and Systems, v. 10, p. 30-37, 2015.